2024 IEEE International Conference on Robotics and Automation (ICRA)
May 13-17, 2024. Yokohama, Japan

2024 IEEE International Conference on Robotics and Automation (ICRA) | 979-8-3503-8457-4/24/$31.00 ©2024 IEEE | DOI: 10.1109/ICRA57147.2024.10611263

A Dual Closed-Loop Control Strategy for Human-Following Robots Respecting Social Space

Jianwei Peng[1*], Zhelin Liao[1*], Zefan Su[1], Hanchen Yao[1], Yadan Zeng[2], and Houde Dai[1], *Senior Member, IEEE*

***Abstract*— Human following for mobile robots has emerged as a promising technique with widespread applications. To ensure psychological comfort while collaborating, coexisting, and interacting with humans, robots need to respect the social space of the target person. In this study, we propose a dual closed-loop human-following control strategy that combines model predictive control (MPC) and impedance control. The outer-loop MPC ensures precise control of the robot's posture while tracking the target person's velocity and direction to coordinate the motion between them. The inner-loop impedance controller is employed to regulate the robot's motion and interaction force with the target person, enabling the robot to maintain a respectful and comfortable distance from the target person. Concretely, the social interaction dynamics characteristics between the robot and the target person are described by human-robot interaction dynamics, which considers the rules of social space. Furthermore, an obstacle avoidance component constructed using behavioral dynamics is integrated into the impedance controller. Experimental results demonstrate the effectiveness of the proposed method in achieving human following and obstacle avoidance without intruding into the intimate zone of the target person.**

I. INTRODUCTION

A wide range of human-robot collaborative applications exist in diverse domains, such as logistics, medical care, and social activities [1]–[3]. Particularly, robots equipped with human-following capabilities can reduce human workloads and enhance overall efficiency [3]. However, it is insufficient to merely treat the target person as a tracking object when a human-following robot coexists and collaborates with a person. Robots are expected to exhibit human-friendly behaviors and adhere to socially acceptable norms, thereby enhancing human comfort and facilitating broader acceptance [4].

Many state-of-the-art human-following control methods [5]–[18] have yield impressive results. For instance, Zhang et al. [5] employed PID control to design a vision-based target-following guide. Similar control methods were also presented in [6]–[8]. Aye et al. [9] and Van et al. [10] extensively investigated fuzzy control-based human-following controllers. Furthermore, Kastner et al. [12] proposed a deep reinforcement learning-based agent for human following in crowded environments. However, these methods concentrate solely on the posture control of the robot relative to the target person, overlooking the critical human factor in human-robot interaction.

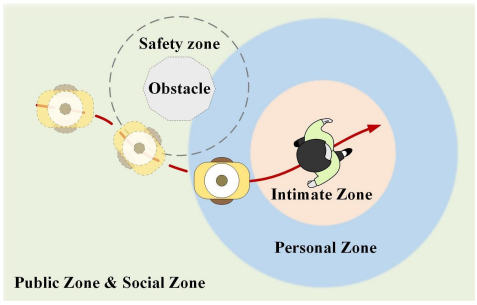

Fig. 1. Diagram of socially accepted human-following behavior. The robot follows the target person from behind and avoids obstacles while refraining from intruding into the target person's intimate zone.

Research on spatiality in social interactions indicates that humans unconsciously maintain appropriate social space between themselves and others during interactions, fostering respect for others and averting discomfort [19]. Proxemic studies by Hall [20] have identified four interpersonal distances that govern social interactions: intimate (0-0.46 m), personal (0.46-1.2 m), social (1.2-3.6 m), and public (>3.6 m). The intimate zone, spanning 0-0.46 m, represents an exceptionally sensitive space where individuals strive to evade encroachment by others. This insight extends to human-robot collaboration, where the robot must recognize and respect the social space, thus aligning with more socially acceptable behavior [21]. Especially, the robot must avoid intruding into the target person's intimate zone [4], as shown in Fig.1.

Correspondingly, Repiso et al. [22] proposed a social force model-based social-awareness navigation framework for accompanying humans that takes into account social space rules. However, methods based on social navigation often involve cumbersome parameter adjustments and could be tricky to migrate onto different robots. Furthermore, Herrera et al. [23] emphasized that ensuring individual comfort requires considering not only social space but also the dynamics during the interaction, i.e., treating these zones as flexible potential areas, enabling the robot to achieve natural and smooth motion for individual comfort. They characterize these dynamics through an impedance control

*Equal contribution. This work was supported by the Quanzhou Science and Technology Project under Grant 2022FX7, and the Open Project Program of Fujian Key Laboratory of Special Intelligent Equipment Measurement and Control, Fujian Special Equipment Inspection and Research Institute, China, FJIES2023KF02. Corresponding authors: Yadan Zeng and Houde Dai. Video demonstration: https://youtu.be/Q1BG2GLAg8c

[1]All authors are with the Quanzhou Institute of Equipment Manufacturing, Fujian Institute of Research on the Structure of Matter, Chinese Academy of Sciences, Jinjiang 362216, China, and also with the Fujian College, University of Chinese Academy of Sciences, Jinjiang 362216, China. Email: pengjianwei20@mails.ucas.ac.cn, 3211239023@fafu.edu.cn, yaohanchen21@mails.ucas.ac.cn, 228527150@fzu.edu.cn, dhd@fjirsm.ac.cn.

[2]Yadan Zeng is with the Robotics Research Centre of the School of Mechanical and Aerospace Engineering, Nanyang Technological University, Singapore. Email: yadan001@e.ntu.edu.sg.

and governed the robot to maintain a comfortable distance from the person. However, this approach lacked consideration for controlling the robot's heading angle and obstacle avoidance, limiting its practicality. Subsequently, Tian et al. [24] designed an impedance human-following controller that included heading angle control and an obstacle avoidance component, effectively addressing the deficiencies of Herrera's method [23]. Nevertheless, this method was only validated through simulation. Impedance control is a typical human-robot interaction control method that enables robots to exhibit compliant behaviors, reduces the uncanny valley effect, and enhances psychological comfort during interactions [25]. However, it has limitations in terms of robustness and accuracy. Additionally, none of the previously mentioned methods can adequately handle the physical constraints of the robot, potentially posing security risks in robot control.

To address these limitation, model predictive control (MPC) is a preferred method due to its inherent advantages, such as the ability to predict future states, generate optimal control actions, handle explicit constraints, and demonstrate excellent robustness. In previous studies [13]–[18], researchers have extensively explored the application of MPC in human-following tasks with commendable performance. However, these methods disregard the target person's interaction experience and the robot's social acceptance. To this end, Sekiguchi et al. [4], [26] adopted MPC to control the relative position of the robot and the target person, ensuring the robot evades intruding into the target person's intimate zone. Nevertheless, this approach assumes that the speed of the target person remains constant, which limits its practicality. Additionally, MPC alone cannot establish compliant interaction between the robot and the target person, resulting in a lack of naturalness and comfort in human-robot interaction.

In response to these challenges, our work incorporates the advantages of impedance control and MPC via a dual closed-loop control structure. The outer-loop MPC ensures precise control of the robot's posture relative to the target person, while tracking the velocity and direction of the target person to coordinate their motion. Additionally, in the inner loop, we design the human-robot interaction dynamics based on social space rules to capture the social repulsion between the robot and the target person. Then, dynamically regulates the robot's motion and interaction force by impedance control to achieve compliant human-following behavior while respecting the target person's social space.

Furthermore, previous studies have often neglected the significance of obstacle avoidance in the human-following task (e.g., [6], [8], [23], [26]). Additionally, research on human-robot interaction has revealed that similarity between robots and humans in low-level behavior patterns can effectively enhance the naturalness of the robot's behavior, thereby enriching the interaction experience for individuals and promoting the social acceptance of robots [27]. Nonetheless, conventional obstacle avoidance methods (e.g., [10], [14]) typically ignore this aspect. Therefore, behavioral dynamics [24], [28] is preferred, which allows the robot to avoid obstacles by emulating human walking behavior.

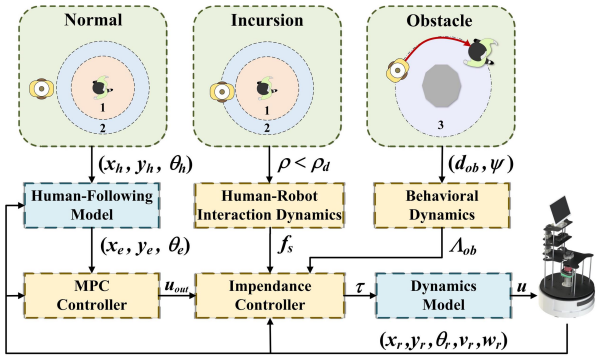

Fig. 2. Overview of the proposed scheme for the human-following control strategy based on MPC and impedance control. Zones 1 and 2 are the intimate zone and threshold zone of the target person, respectively. Zone 3 is the safe area of the obstacle.

The main contributions are summarized as follows:

1) Developing a dual closed-loop human-following controller involves an outer-loop model predictive controller for human following, a social space rules-based human-robot interaction dynamics for generating interaction force, and an inner-loop impedance controller for regulating robot motion and interaction force.
2) Integrating behavioral dynamics with the impedance controller as an obstacle avoidance component. The robot's behaviors hence are further refined, rendering the robot more natural and reflective of human-like navigation and interaction.

II. System Overview

As illustrated in Fig. 2, the proposed human-following control scheme primarily consists of a dual closed-loop human-following controller, human-robot interaction dynamics, and behavioral dynamics. The dual closed-loop controller, combining MPC and impedance control, is responsible for executing the human-following tasks. The outer-loop MPC governs the robot's positional deviation to follow the target person, while simultaneously tracking the target person's velocity and direction to ensure motion coordination between the robot and the target person. Utilizing human-robot interaction dynamics, a dynamic virtual interaction force is established between the robot and the target person. When the robot enters the threshold zone of the target person, a repulsive interaction force is generated and applied to the robot. Subsequently, the inner-loop impedance controller enables the robot to maintain a respectful distance from the target person by dynamically regulating the robot's motion and the virtual interaction force. This strategy prevents the robot from intruding into the target person's intimate zone and enhances the compliance of the human-following control. Additionally, behavioral dynamics is integrated into the impedance controller as an obstacle avoidance component, enabling the robot to autonomously navigate an obstacle avoidance trajectory without prior planning. Notably, we employ an electromagnetic tracking module to directly acquire the position and orientation of the target person and a LiDAR to detect obstacles, both of which are introduced in Section V. The system operates in closed loop with perception and control updates at 20 Hz.

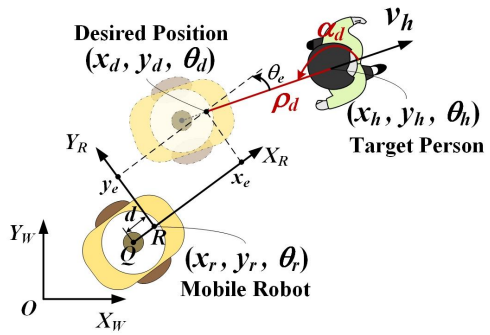

Fig. 3. Diagram of the human-following system model. R is the center of mass, Q is the center of the wheel axis, and d is the distance between the robot's wheel axis and its centroid.

III. Problem Formulation

A. Robot Motion Modeling

A differential-driven mobile robot is employed as the human-following robot. Consequently, the robot's kinematics can be described as $\dot{x}_r = v_r cos\theta_r$, $\dot{y}_r = v_r sin\theta_r$, $\dot{\theta}_r = w_r$, where (x_r, y_r) represents the robot's position, and θ_r denotes its orientation. v_r and w_r are the linear and angular velocities of the robot, respectively. Furthermore, the dynamics of the human-following robot can be defined according to [29], as

$$\bar{M}\dot{u} + \bar{C}u = \bar{B}\tau, \tag{1}$$

where $u = [v_r, w_r]^T$ is the control input. τ is the robot's driving torques. J_r and m are the rotational inertia and the mass of the robot, respectively. r is the radius of the wheels, and l is the distance between the vehicle's wheels,

$$\bar{M} = \begin{bmatrix} m & 0 \\ 0 & J_r \end{bmatrix}, \quad \bar{C} = 0^{2\times 2}, \quad \bar{B} = \frac{1}{r}\begin{bmatrix} 1 & 1 \\ l & -l \end{bmatrix}.$$

B. Human-Following System Model

The system schematic of human following is illustrated in Fig. 3. The state of the target person is denoted as $[x_h, y_h, \theta_h, v_h, w_h]^T$, where (x_h, y_h) and θ_h are the position and orientation of the target person, respectively. v_h and w_h represent the forward and turning velocities of the target person, respectively. The desired position of the human-following robot is denoted as $[x_d, y_d, \theta_d]^T$, determined by the desired relative position and orientation relationship between the target person and the robot, as

$$\begin{cases} x_d = x_h + \rho_d cos(\alpha_d + \theta_h) \\ y_d = y_h + \rho_d sin(\alpha_d + \theta_h) \\ \theta_d = \theta_h + \beta_d \end{cases}, \tag{2}$$

where $[\rho_d, \alpha_d, \beta_d]^T$ is the desired human-following system state, signifying the separation, bearing, and orientation between the target person and the robot, respectively. Then, we can obtain the tracking error model [30]

$$\dot{X}_e = \begin{bmatrix} 0 & w_h & 0 \\ -w_h & 0 & v_h \\ 0 & 0 & 0 \end{bmatrix}\begin{bmatrix} x_e \\ y_e \\ \theta_e \end{bmatrix} + \begin{bmatrix} 1 & 0 \\ 0 & 0 \\ 0 & 1 \end{bmatrix} u_e, \tag{3}$$

where $X_e = [x_e, y_e, \theta_e]^T$ is the robot's position error in the robot body-fixed frame, $x_e = x_r - x_d$, $y_e = y_r - y_d$, $\theta_e = \theta_r - \theta_d$, and $u_e = [v_h cos\theta_e - v_r, w_h - w_r]^T$.

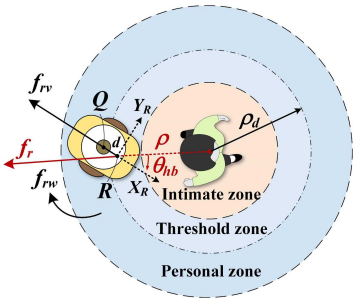

Fig. 4. Diagram of human-robot interaction dynamics.

Subsequently, we can obtain the time-varying discrete linearized error model, as

$$X_e(k+1) = AX_e(k) + Bu_e(k), \tag{4}$$

where T is the sample period,

$$A = \begin{bmatrix} 1 & Tw_h(k) & 0 \\ -Tw_h(k) & 1 & Tv_h(k) \\ 0 & 0 & 1 \end{bmatrix}, \quad B = \begin{bmatrix} T & 0 \\ 0 & 0 \\ 0 & T \end{bmatrix}.$$

C. Human-Robot Interaction Dynamics

As depicted in Fig. 4, the human-robot interaction dynamics is developed based on social space rules [20], [31]. It utilizes non-physical forces to characterize the dynamic interaction relationship between the robot and the target person, assuming the existence of a hypothetical potential field within the person's intimate zone. If the robot enters this zone during the human-following task, a repulsive force can push the robot away from the intimate zone.

To ensure human comfort, we design a threshold zone slightly larger than the intimate zone, with the desired distance of the robot from the target person (ρ_d) set as the radius of the threshold zone. As the relative distance ρ between the robot and the target person becomes less than ρ_d, a repulsive interaction force is applied, pushing the robot away from that zone. The virtual interaction force can be given by [23]

$$f_r = \begin{cases} \gamma \frac{e^{-\frac{\rho^n}{\rho_d}} - e^{-\rho_d^{n-1}}}{1 - e^{-\rho_d^{n-1}}}, & \rho \le \rho_d \\ 0, & \rho > \rho_d \end{cases}, \tag{5}$$

where γ is denoted as gain, n is the order, and ρ_d is the desired distance and the range of the interaction force. Then, f_r can be composed as

$$f_s = [-f_r cos\theta_{hb}, -f_r d sin\theta_{hb}]^T, \tag{6}$$

where $f_s = [f_{rv}, f_{rw}]^T$ represents the components of f_r in the forward and rotational directions of the robot, respectively. θ_{hb} is the azimuth angle of the target person in the robot body-fixed frame.

IV. Human-Following Control Strategy

As shown in Fig. 2, the proposed human-following control strategy consists of a dual closed-loop structure based on MPC and impedance control. Besides, the proposed method incorporates behavioral dynamics for obstacle avoidance.

A. Outer-Loop Model Predictive Controller

The task of MPC is to control the posture of the robot relative to the target person while tracking the velocity and direction of the target person to coordinate the motion between them, i.e., $\lim_{t\to\infty}|X_e|=0, \lim_{t\to\infty}|u_e|=0$. Thus, the cost function of MPC can be formulated as

$$J=\sum_{i=1}^{Np}\|X_e(k+i|k)\|_q^2+\sum_{i=0}^{Nc-1}\|u_e(k+i|k)\|_r^2, \tag{7}$$

where $X_e(k+i|k)$ represents the position and direction deviation of the robot in the prediction horizon, $u_e(k+i|k)$ denotes the control input in the control horizon, q and r are the weight matrices, N_p and N_c are the prediction horizon and control horizon, respectively.

To ensure smoothness of control and to satisfy the physical constraints of the robot, we impose constraints as $u_{min}\le u\le u_{max}$ and $u_{e(min)}\le u_e(k)\le u_{e(max)}$, respectively. Subsequently, the cost function (7) can be reformulated in a normal quadratic programming format, as

$$\begin{aligned}&\min_{(X_e,U)} J(k)=\frac{1}{2}U(k)^THU(k)+X_e(k)^TEU(k) \\ &\text{s.t.}\quad u_{min}\le u(k)\le u_{max}, u_{e(min)}\le u_e(k)\le u_{e(max)},\end{aligned} \tag{8}$$

where $U(k)=[u_e(k|k),...,u_e(k+N_c-1|k)]^T$,

$$E=\Phi^TQ\Theta, H=\Theta^TQ\Theta+R, Q=\bigoplus_{i=1}^{N_p}q(i), R=\bigoplus_{i=1}^{N_c-1}r(i),$$

$$\Phi=\begin{bmatrix}A\\A^2\\...\\A^{N_p}\end{bmatrix}, \Theta=\begin{bmatrix}B & 0 & 0 & \cdots & 0\\ AB & B & 0 & \cdots & 0\\ \vdots & \vdots & \vdots & \ddots & \vdots\\ A^{N_c-1}B & A^{N_c-2}B & A^{N_c-3}B & \cdots & B\end{bmatrix}.$$

Solve (8) obtain the optimal control sequence $U^*(k)$ and use its first element as the control output $u_e^*(k)$. Then, we can obtain model predictive control law of the outer-loop, as

$$u_{out}(k|k)=u_d(k|k)+u_e^*(k). \tag{9}$$

B. Inner-Loop Impedance Controller

The goal of the inner-loop impedance controller is to establish a dynamic regulation between the robot's motion and the social force interacting with the target person. The optimal output of the MPC serves as the reference input for the inner-loop controller. The impedance control law is given by [32]

$$\tilde{I}\ddot{\zeta}_e+\tilde{B}\dot{\zeta}_e+\tilde{K}\zeta_e=f_s, \tag{10}$$

where $\zeta_e:=[s_v-s_d,\theta_r-\theta_d]^T$ denotes the displacement and directional deviation of the robot, s_v and s_d represent the real displacement and desired displacement of the robot, respectively. $I=diag(i,i)$, $B=diag(b,b)$, and $K=diag(k,k)$ are inertia, damping, and elastic matrix, respectively. f_s, obtained from (6), is the virtual interaction force between the robot and the target person.

Subsequently, according to the robot dynamics (1) and the human-robot interaction dynamics (5), the inner-loop impedance control law can be obtained as

$$\tau=\bar{B}^{-1}\bar{M}(\dot{u}_d+I^{-1}(f_s-B\dot{\zeta}_e-K\zeta_e)). \tag{11}$$

C. Obstacle Avoidance Based on Behavioral Dynamics

The principle of behavioral dynamics is to emulate human walking behavior, i.e., humans will adjust their walking direction in advance to avoid obstacles and generally will not have to adjust their forward speed [24], [28]. Therefore, this method achieves obstacle avoidance by adjusting the angular velocity of the robot. Let d_{ob} be the distance from the robot to the obstacle and d_s be the safe distance, then we have:

$$\Lambda_{ob}=\begin{cases}-k_0\psi e^{-c_1|\psi|}e^{-c_2d_{ob}}, & d_{ob}\le d_s\\ 0, & d_{ob}>d_s\end{cases}, \tag{12}$$

where Λ_{ob} is the output of the obstacle avoidance component, ψ is the orientation angle of the obstacle relative to the robot, $k_0>0$, $c_1>0$, and $c_2>0$ are gains.

Thus, we can obtain the obstacle avoidance control input generated by $i-th$ obstacle, i.e., $\dot{u}_{ob}^i=\left[0,\Lambda_{ob}^i\right]^T$. Assuming that N_{ob} is the number of obstacles, the inner-loop impedance controller based on behavioral dynamics can be written as

$$\tau=\bar{B}^{-1}\bar{M}(\dot{u}_d+I^{-1}(f_s-B\dot{\zeta}_e-K\zeta_e)+\sum_{i=1}^{N_{ob}}\dot{u}_{ob}^i). \tag{13}$$

V. Simulations and Experiments

A. Experimental Conditions

1) Experimental Setup: The simulation of the human-following task was conducted in MATLAB 2021b. To quickly validate the effectiveness of the proposed method in a real-world experiment, we established a master-slave network by connecting MATLAB to Robot Operating System (ROS, noetic), as depicted in Fig. 6. The control algorithm runs in MATLAB, and control commands are transmitted from ROS to the robot's actuator. Concurrently, ROS provides sensor data to MATLAB. The optimization problem in MPC is solved using quadprog. Specifically, we employ an electromagnetic tracking module (EMTM[1]) to directly acquire the position and orientation of the target person and a LiDAR to detect obstacles.

2) Evaluation Metrics: To quantitatively evaluate the control strategy, we have defined the following metrics from the control perspective (a small value is preferred). **a) Uncomfortable Time** $T_{uc}=\sum_{t=0}^{T_{task}}\delta_t$, $\delta_t=\begin{cases}0 & 0.6\le\rho\le1.2\\ T & \rho<0.6 \quad or \quad \rho>1.2\end{cases}$ evaluates the robot's ability to refrain from intruding into the target person's intimate zone [4], where T_{task} is the duration of a task. **b) Motion Smoothness** $\boldsymbol{M}_{sm}=1/T_{task}\sum_{t=0}^{T_{task}}\Delta u$ measures the smoothness of the robot's motion, where $\Delta u=[\Delta v,\Delta w]^T$ is the control input increments. **c) Tracking Error** $\boldsymbol{E}_{ts}=\sqrt{1/T_{task}\sum_{t=0}^{T_{task}}(\boldsymbol{\zeta}-\boldsymbol{\zeta_d})^2}$ assesses the tracking accuracy of the robot, where $\boldsymbol{\zeta}:=[\rho,\alpha,\beta]^T$ is the system state.

[1]Amfitech. https://www.amfitech.dk/

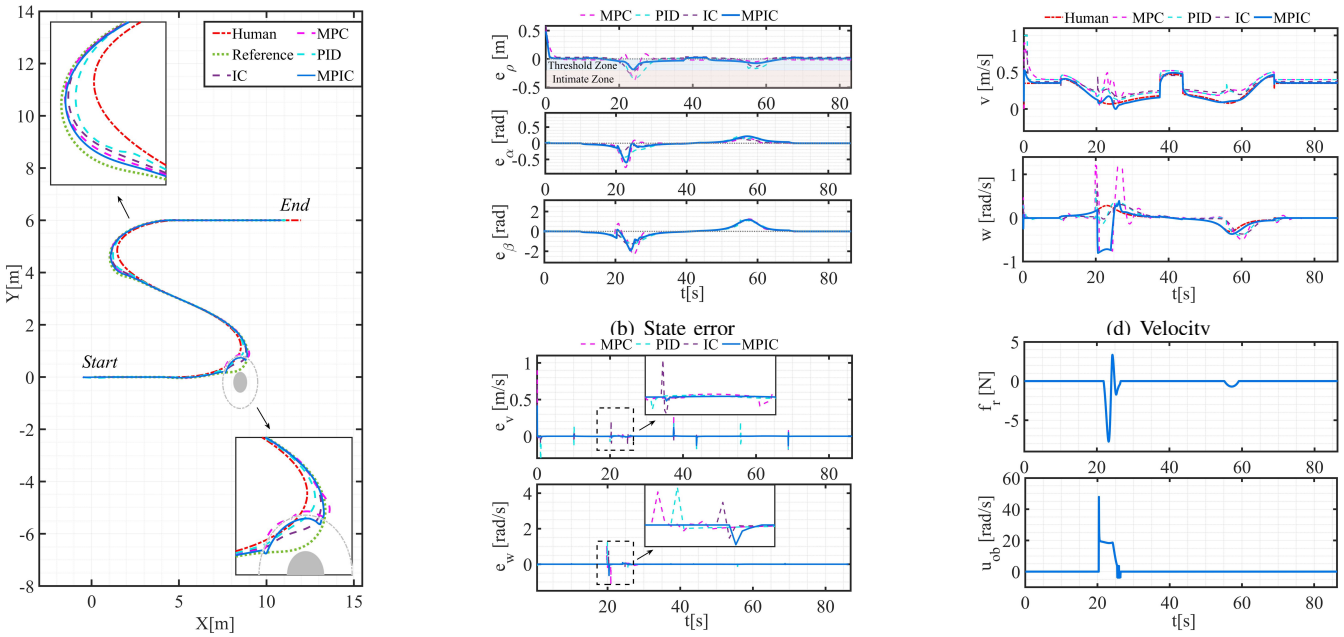

Fig. 5. Simulation of human-following task and comparison with PID, impedance control (IC), and MPC. MPIC represents our proposed method. The green dotted line in (a) is the desired trajectory of the robot, which is obtained from (2). Gray solid circle and gray dotted line in (a) represent the obstacle and safety zone, respectively. In (b), $[e_\rho, e_\alpha, e_\beta]^T := [\rho - \rho_d, \alpha - \alpha_d, \beta - \beta_d]^T$, and the blue zone and the pink zone represent the threshold zone and intimate zone of the target person, respectively.

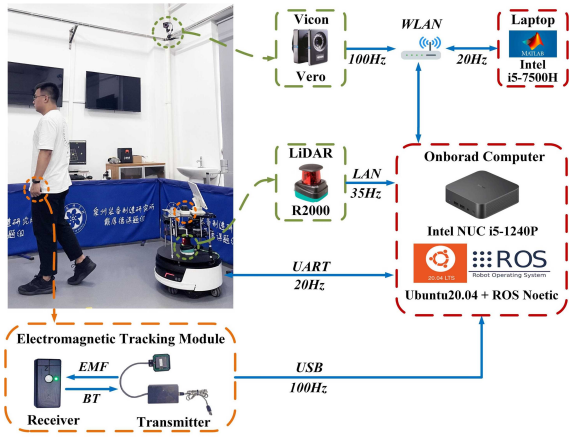

Fig. 6. Experimental setup. EMF: electromagnetic field, BT: Bluetooth. The EMTM transmitter is mounted on the robot. The receiver is worn by the target person. World coordinate determined by odometry. Vicon is utilized to capture the trajectory of the target person and the robot.

TABLE I

QUANTITATIVE RESULTS OF SIMULATIONS

Methods	T_{uc} [s]	$\boldsymbol{M}_{sm}$		$\boldsymbol{E}_{ts}$		
		v[m/s]	w[rad/s]	ρ [m]	α [rad]	β [rad]
MPIC	**0.0**	0.162	**0.248**	**0.074**	**0.098**	**0.435**
MPC	1.6	0.286	0.471	0.158	0.204	0.544
IC	1.1	**0.145**	0.251	0.452	0.365	0.861
PID	3.8	0.263	0.513	0.325	0.294	0.692

B. Simulation Results

To validate the effectiveness and superiority of our proposed method, we conducted a simulation experiment. As illustrated in Fig. 5, we compared our proposed method with PID, impedance control (IC), and MPC. The blue curves (MPIC) in Fig. 5 represent the results obtained by our proposed method. At $t = 20s$, as shown in Fig. 5, the robot approached the target person's intimate zone while bypassing the obstacle. Notably, our proposed method successfully avoided intruding into the target person's intimate zone. This accomplishment is evident in the tracking error e_ρ in Fig. 5(b) and the interaction force f_r in Fig. 5(e). Upon entering the threshold zone of the target person, the robot experienced a repulsive interaction force f_r, preventing it from intruding into the intimate zone. In contrast, all other methods resulted in encroachment upon the target person's intimate zone. Additional, as indicated by t_{uc} in Table I, only MPIC is 0, which means our method enables the robot to avoid psychological discomfort by respecting the target person's social space, a feat that the other methods failed to achieve.

Furthermore, as illustrated in Fig. 5(c) and Fig. 5(d), our proposed method provided stable and smooth velocity tracking of the target person. In Table I, the motion smoothness $\boldsymbol{M}_{sm}$ of our method is comparable to impedance control but superior to other methods. This characteristic ensures effective motion coordination between the robot and the target person, improving the stability of the human-following formation. Moreover, our method achieves smaller tracking errors compared to the other methods. Notably, the error of β is more obvious partly due to the effect of obstacle avoidance and target person's motion variations, on the other hand, the control priority of orientation is lower, and its weight is smaller. These results indicates that our method possesses the compliance of impedance control coupled with the control accuracy and robustness of MPC.

C. Real-World Experiment Results

To assess the practical applicability of our proposed method, we conducted two sets of experiments using the setup depicted in Fig. 6. The quantitative results of these

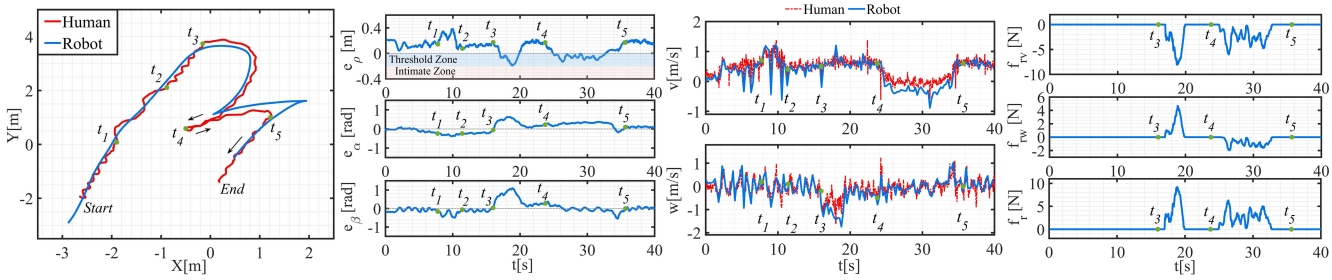

(a) Trajectories (b) State error (c) Velocity (d) Interaction force

Fig. 7. Human-following experiment with motion mutations in the target person. The target person suddenly accelerates at t_1 and decelerates at t_2, turns 180° at t_3, briefly steps back at t_4 to approach the robot, and resumes forward at t_5. The black arrow in (a) is the direction of the target person's motion.

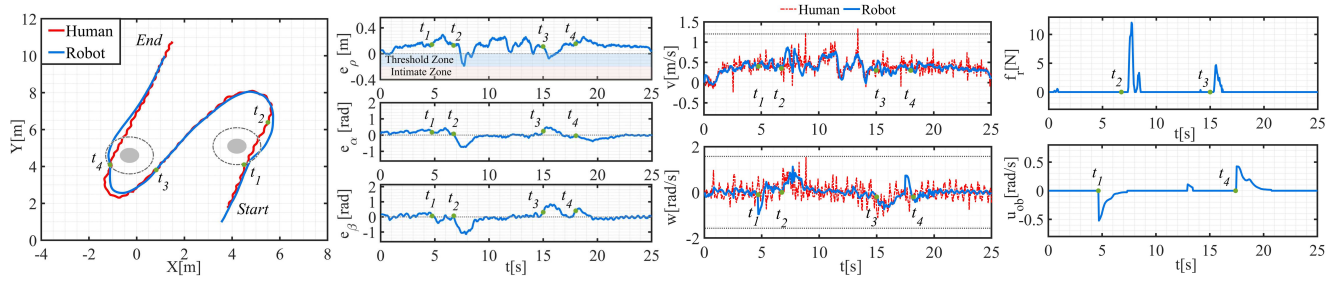

(a) Trajectories (b) State error (c) Velocity (d) f_r and u_{ob}

Fig. 8. Experiment for human-following and obstacle avoidance. Gray solid circle and gray dotted line in (a) are obstacles and the safety zone, respectively. The blue zone and pink zone in (b) are the threshold zone and intimate zone of the target person, respectively.

TABLE II

QUANTITATIVE RESULTS OF REAL-WORLD EXPERIMENTS

Experiment	T_{uc} [s]	$\boldsymbol{M}_{sm}$		$\boldsymbol{E}_{ts}$		
		v[m/s]	w[rad/s]	ρ [m]	α [rad]	β [rad]
Motion mutations	0.0	0.292	0.314	0.206	0.291	0.506
Obstacle avoidance	0.0	0.137	0.262	0.158	0.244	0.412

evaluations are summarized in Table II. In the first set of experiments, we introduced variations in the velocity and direction of the target person at t_1 and t_3, respectively. As illustrated in Fig. 7(b) and Fig. 7(c), the robot effectively adapted to these motion changes and maintained smooth velocity tracking. Even in scenarios with significant deviations in the system state due to the target person's motion mutations, our system rapidly reconverged while remaining stable. Moreover, when the target person executed a 180° turn at t_3 and briefly stepped back at t_4 to approach the robot, the robot inadvertently entered the target person's threshold zone. However, the robot was promptly repelled by a repulsive interaction force, preventing further encroachment into the target person's intimate zone, as demonstrated in Fig. 7(b) and Fig. 7(d).

In the second set of experiments, the trajectory of the target person closely resembled the simulation shown in Fig. 5. As depicted in Fig. 8, the robot consistently followed the target person, smoothly tracking the target person's velocity while effectively avoiding obstacles. When encountering obstacles and in response to abrupt changes in the target person's motion, the system state experienced significant deviations. However, the proposed method exhibited remarkable adaptability, quickly re-converging the system to the desired state. Additionally, when interaction forces were at play, the robot demonstrated human-friendly behaviors by respecting the target person's social space. The robot successfully avoided intruding into the target person's intimate zone, as shown in Fig. 8(b) and Fig. 8(d), which is also confirmed by $T_{uc} = 0$ in Table II. This capability enhanced the overall comfort and acceptance of the robot during human-robot interactions. These results affirm the effectiveness and robustness of our proposed method in real-world scenarios, highlighting its practical potential in human-robot collaboration.

VI. CONCLUSIONS

This study presents an effective dual closed-loop human-following control strategy that enables the robot to respect the target person's social space, thereby improving the target person's comfort and promoting the robot's social acceptance. The MPC-based outer-loop controller ensures accurate and stable robot posture control and motion coordination with the target person. Simultaneously, the human-robot interaction dynamics based on social space rules is utilized to capture the social repulsion between the robot and the target person. The inner-loop impedance controller is designed to dynamically regulate the robot's motion and interaction force. Thus, the robot maintains a comfortable and respectful interaction distance with the target person while improving control compliance. Moreover, the impedance controller integrates behavioral dynamics as an obstacle avoidance component, enabling the robot to emulate the obstacle avoidance behavior of humans. Experimental results demonstrate the effectiveness and superiority of the proposed human-following control strategy. The proposed approach in this study promises to advance human-robot interaction by making robots more adaptable and respectful in their interactions with humans. In the future, we will consider the feelings of pedestrians when following in crowded environments to improve the social awareness of human-following robots.

REFERENCES

[1] S. Li, K. Milligan, P. Blythe, Y. Zhang, S. Edwards, N. Palmarini, L. Corner, Y. Ji, F. Zhang, and A. Namdeo, "Exploring the role of human-following robots in supporting the mobility and wellbeing of older people," *Scientific Reports*, vol. 13, no. 1, p. 6512, 2023.

[2] M. J. Islam, J. Hong, and J. Sattar, "Person-following by autonomous robots: A categorical overview," *The International Journal of Robotics Research*, vol. 38, no. 14, pp. 1581–1618, 2019.

[3] S. S. Honig, T. Oron-Gilad, H. Zaichyk, V. Sarne-Fleischmann, S. Olatunji, and Y. Edan, "Toward socially aware person-following robots," *IEEE Transactions on Cognitive and Developmental Systems*, vol. 10, no. 4, pp. 936–954, 2018.

[4] S. Sekiguchi, A. Yorozu, K. Kuno, M. Okada, Y. Watanabe, and M. Takahashi, "Uncertainty-aware non-linear model predictive control for human-following companion robot," in *2021 IEEE International Conference on Robotics and Automation (ICRA)*. IEEE, 2021, pp. 8316–8322.

[5] M. Zhang, X. Liu, D. Xu, Z. Cao, and J. Yu, "Vision-based target-following guider for mobile robot," *IEEE Transactions on Industrial Electronics*, vol. 66, no. 12, pp. 9360–9371, 2019.

[6] C. Wu, B. Tao, H. Wu, Z. Gong, and Z. Yin, "A uhf rfid-based dynamic object following method for a mobile robot using phase difference information," *IEEE Transactions on Instrumentation and Measurement*, vol. 70, pp. 1–11, 2021.

[7] A. Wang, Y. Makino, and H. Shinoda, "Machine learning-based human-following system: Following the predicted position of a walking human," in *2021 IEEE International Conference on Robotics and Automation (ICRA)*. IEEE, 2021, pp. 4502–4508.

[8] H. Yao, H. Dai, E. Zhao, P. Liu, and R. Zhao, "Laser-based side-by-side following for human-following robots," in *2021 IEEE/RSJ International Conference on Intelligent Robots and Systems (IROS)*. IEEE, 2021, pp. 2651–2656.

[9] Y. Y. Aye, K. Thiha, M. M. M. Pyu, and K. Watanabe, "A deep neural network based human following robot with fuzzy control," in *2019 IEEE International Conference on Robotics and Biomimetics (ROBIO)*. IEEE, 2019, pp. 720–725.

[10] N. Van Toan, M. Do Hoang, P. B. Khoi, and S.-Y. Yi, "The human-following strategy for mobile robots in mixed environments," *Robotics and Autonomous Systems*, vol. 160, p. 104317, 2023.

[11] J. Peng, Z. Liao, Z. Su, H. Yao, Y. Zeng, and H. Dai, "Human-robot interaction dynamics-based impedance control strategy for enhancing social acceptance of human-following robot," in *2023 China Automation Congress (CAC)*. IEEE, 2023.

[12] L. Kästner, B. Fatloun, Z. Shen, D. Gawrisch, and J. Lambrecht, "Human-following and-guiding in crowded environments using semantic deep-reinforcement-learning for mobile service robots," in *2022 International Conference on Robotics and Automation (ICRA)*. IEEE, 2022, pp. 833–839.

[13] S. Hong, J. Lu *et al.*, "A transient response adjustable mpc for following a dynamic object," in *2023 American Control Conference (ACC)*. IEEE, 2023, pp. 1434–1439.

[14] A. K. Ashe and K. M. Krishna, "Maneuvering intersections & occlusions using mpc-based prioritized tracking for differential drive person following robot," in *2021 IEEE 17th International Conference on Automation Science and Engineering (CASE)*. IEEE, 2021, pp. 1352–1357.

[15] N. Hirose, R. Tajima, and K. Sukigara, "Mpc policy learning using dnn for human following control without collision," *Advanced Robotics*, vol. 32, no. 3, pp. 148–159, 2018.

[16] S. Yan, J. Tao, J. Huang, and A. Xue, "Model predictive control for human following rehabilitation robot," in *2019 IEEE International Conference on Advanced Robotics and its Social Impacts (ARSO)*. IEEE, 2019, pp. 369–374.

[17] Y. Zhang, J. Huang, J. Yu, Y. Zhu, and Y. Hasegawa, "Relative-posture-fixed model predictive human-following control with visibility constraints in obstacle environments," in *2023 International Conference on Advanced Robotics and Mechatronics (ICARM)*. IEEE, 2023, pp. 959–964.

[18] J. Peng, Z. Liao, H. Yao, Z. Su, Y. Zeng, and H. Dai, "Mpc-based human-accompanying control strategy for improving the motion coordination between the target person and the robot," in *2023 IEEE/RSJ International Conference on Intelligent Robots and Systems (IROS)*. IEEE, 2023, pp. 7969–7975.

[19] H. Hüttenrauch, K. S. Eklundh, A. Green, and E. A. Topp, "Investigating spatial relationships in human-robot interaction," in *2006 IEEE/RSJ International Conference on Intelligent Robots and Systems (IROS)*. IEEE, 2006, pp. 5052–5059.

[20] E. T. Hall, "A system for the notation of proxemic behavior," *American anthropologist*, vol. 65, no. 5, pp. 1003–1026, 1963.

[21] M. R. Batista, D. G. Macharet, and R. A. Romero, "A study on the effect of human proxemics rules in human following by a robot team," in *2017 Latin American Robotics Symposium (LARS) and 2017 Brazilian Symposium on Robotics (SBR)*. IEEE, 2017, pp. 1–6.

[22] E. Repiso, A. Garrell, and A. Sanfeliu, "Adaptive side-by-side social robot navigation to approach and interact with people," *International Journal of Social Robotics*, vol. 12, pp. 909–930, 2020.

[23] D. Herrera, F. Roberti, M. Toibero, and R. Carelli, "Human interaction dynamics for its use in mobile robotics: Impedance control for leader-follower formation," *IEEE/CAA Journal of Automatica Sinica*, vol. 4, no. 4, pp. 696–703, 2017.

[24] H. Tian and X. Ma, "Behavioral dynamics-based impedance control for collision avoidance of human-following robots," in *2022 IEEE International Conference on Real-time Computing and Robotics (RCAR)*. IEEE, 2022, pp. 349–354.

[25] P.-Y. Oudeyer, O. Ly, and P. Rouanet, "Exploring robust, intuitive and emergent physical human-robot interaction with the humanoid robot acroban," in *2011 11th IEEE-RAS International Conference on Humanoid Robots*. IEEE, 2011, pp. 120–127.

[26] S. Sekiguchi, A. Yorozu, K. Kuno, M. Okada, Y. Watanabe, and M. Takahashi, "Human-friendly control system design for two-wheeled service robot with optimal control approach," *Robotics and Autonomous Systems*, vol. 131, p. 103562, 2020.

[27] Y. Gao and C.-M. Huang, "Evaluation of socially-aware robot navigation," *Frontiers in Robotics and AI*, vol. 8, p. 721317, 2022.

[28] B. R. Fajen and W. H. Warren, "Behavioral dynamics of steering, obstable avoidance, and route selection." *Journal of Experimental Psychology: Human Perception and Performance*, vol. 29, no. 2, p. 343, 2003.

[29] R. Fierro and F. L. Lewis, "Control of a nonholomic mobile robot: Backstepping kinematics into dynamics," *Journal of robotic systems*, vol. 14, no. 3, pp. 149–163, 1997.

[30] G. Klančar and I. Škrjanc, "Tracking-error model-based predictive control for mobile robots in real time," *Robotics and autonomous systems*, vol. 55, no. 6, pp. 460–469, 2007.

[31] M. L. Walters, K. Dautenhahn, S. N. Woods, K. L. Koay, R. Te Boekhorst, and D. Lee, "Exploratory studies on social spaces between humans and a mechanical-looking robot," *Connection Science*, vol. 18, no. 4, pp. 429–439, 2006.

[32] N. Hogan, "Impedance control: An approach to manipulation," in *1984 American control conference*. IEEE, 1984, pp. 304–313.